PHYSICAL REVIEW D **84,** 074011 (2011)

Constraints on the light pseudoscalar meson distribution amplitudes from their meson-photon transition form factors

Xing-Gang Wu*

Department of Physics, Chongqing University, Chongqing 401331, People's Republic of China

Tao Huang†

Institute of High Energy Physics and Theoretical Physics Center for Science Facilities, Chinese Academy of Sciences, Beijing 100049, People's Republic of China

(Received 22 June 2011; published 10 October 2011)

The meson-photon transition form factors $\gamma\gamma^* \to P$ (P stands for π, η and η') provide strong constraints on the distribution amplitudes of the pseudoscalar mesons. In this paper, these transition form factors are calculated under the light-cone perturbative QCD approach, in which both the valence and nonvalence quarks' contributions have been taken into consideration. To be consistent, a unified wave function model is adopted to analyze these form factors. It is shown that with the proper charm component $f^c_{\eta'} \sim -30$ MeV and a moderate DA with $B \sim 0.30$, the experimental data on $Q^2F_{\eta\gamma}(Q^2)$ and $Q^2F_{\eta'\gamma}(Q^2)$ in the whole Q^2 region can be explained simultaneously. Furthermore, a detailed discussion on the form factors' uncertainties caused by the constituent quark masses m_q and m_s, the parameter B, the mixing angle ϕ, and $f^c_{\eta'}$ are presented. It is found that, by adjusting these parameters within their reasonable regions, one can improve the form factor to a certain degree but cannot solve the puzzle for $Q^2F_{\pi\gamma}(Q^2)$, especially to explain the behavior of the $\pi - \gamma$ form factor within the whole Q^2 region consistently. We hope further experimental data on these form factors in the large Q^2 region can clarify the present situation.

DOI: 10.1103/PhysRevD.84.074011 PACS numbers: 12.38.Bx, 12.38.−t, 14.40.Be

I. INTRODUCTION

The distribution amplitude (DA) is the key factor for exclusive processes. Usually, the DAs of the light pseudoscalar mesons can be expanded in Gegenbauer polynomials, and their corresponding Gegenbauer moments have been studied by various groups (cf. Refs. [1–9]). However, there is no definite conclusion on whether the shape of the DA is in an asymptotic form [10] or in a more broad form [11].

The light pseudoscalar meson-photon transition form factor $F_{P\gamma}(Q^2)$ that describes the effect of the strong interaction on $\gamma\gamma^* \to P$ transition (P stands for π, η, and η') provides a good platform for studying the leading-twist DA, since it contains only one bound state and the power-suppressed light meson's higher helicity and higher twist structures usually give negligible contributions. One can extract useful information on the leading-twist DA by comparing the theoretical estimation on $F_{P\gamma}(Q^2)$ with the corresponding experimental data.

Based on the CELLO, CLEO, and *BABAR* data on $\gamma\gamma^* \to \pi$ [12–14], many people have discussed the properties of a pion DA [15–28]. A DA as described by Chernyak and Zhitnitsky [11] (CZ-like DA) or even a flat DA [15] can explain the large Q^2 behavior shown by the *BABAR* data [14]; however, the theoretical estimation on the form factor with a CZ-like or flat DA will always be lower than the experimental results in a small Q^2 region [22]. While, by taking the nonvalence quark parts into consideration and by setting the second pion moment $a_2^\pi(\mu_0^2)$ around 0.35, one can explain the behavior in a small Q^2 region well, a somewhat large discrepancy emerges, however, in the high Q^2 region if the *BABAR* data are confirmed [28]. A reasonable theoretical estimation on the form factor should explain the form factor's behavior in both the lower and higher Q^2 regions consistently. And one should find a way to compare the experiment results on the form factor to determine which DA shape is more suitable.

Moreover, the experimental data on $\gamma\gamma^* \to \eta$ or η' transition [12,13,29–35], especially the new *BABAR* results within the region of $[4, 40]$ GeV^2 [36], can provide further constraints on the pseudoscalar meson's DA [37–43]. Then we have three pseudoscalar meson-photon transition form factors $F_{P\gamma}(Q^2)$ to constrain the light meson's wave function (WF) and DA parameters. Because of η and η' mixing, their condition is somewhat more difficult than the pionic case. Two mixing schemes are adopted in the literature, and even though their mixing parameters can be related through the correlation given by Refs. [44,45], there are differences in dealing with certain processes. One mixing scheme is based on the flavor singlet η_1 and octet η_8, under which one usually introduces two mixing angles θ_1 and θ_8 and adopts the same DA for η_1 and η_8 [38–43]. In the present paper, we adopt the simpler quark-flavor mixing scheme [44], which is based on the quark-flavor basis η_q and η_s, and only one mixing angle ϕ is

*wuxg@cqu.edu.cn
†huangtao@ihep.ac.cn

introduced. Since η_q and η_s have similar structure as that of a pion, it is natural to adopt the same WF model for π, η_q, and η_s. We adopt the WF model raised by Ref. [28] for our discussion, since by setting the parameter B properly, we can obtain different DA behavior from asymptoticlike (AS-like) to CZ-like naturally, and then we can determine which behavior is more suitable for simultaneously explaining the experimental data of these form factors.

The paper is organized as follows. In Sec. II, we outline our calculation techniques for the transition form factors $F_{P\gamma}(Q^2)$, where the mixing scheme for η and η', a uniform WF model for the mesons, and the analytic formulas for deriving $F_{P\gamma}(Q^2)$ are presented. In Sec. III, we present the numerical results and discuss the uncertainty sources. Section IV is reserved for a summary.

II. BASIC FORMULAS FOR THE FORM FACTORS $F_{P\gamma}(Q^2)$

In this section, we present necessary formulas for the transition form factors $F_{P\gamma}(Q^2)$. First, we define the physical meson states η and η' under the quark-flavor basis, and then we give the uniform WF model for the mentioned pseudoscalar mesons. Finally, we present the form factor with the valence quark contribution calculated up to next-to-leading order (NLO), together with an estimation of the nonvalence quark state's contributions.

A. η and η' defined under the quark-flavor basis

The physical meson states η and η' are related to the orthogonal states η_q and η_s through an orthogonal transformation

$$\begin{pmatrix} |\eta\rangle \\ |\eta'\rangle \end{pmatrix} = U(\phi) \begin{pmatrix} |\eta_q\rangle \\ |\eta_s\rangle \end{pmatrix}, \qquad U(\phi) = \begin{pmatrix} \cos\phi & -\sin\phi \\ \sin\phi & \cos\phi \end{pmatrix}, \tag{1}$$

where ϕ is the mixing angle. Here, we adopt a single mixing angle scheme that attributes $SU_f(3)$ breaking to the Okubo-Zweig-Iizuka–violating contribution [44]. In the quark-flavor basis, the two orthogonal states $|\eta_q\rangle$ and $|\eta_s\rangle$ are defined in a Fock-state description, $|\eta_q\rangle = \Psi_{\eta_q} \frac{|u\bar{u}+d\bar{d}\rangle}{\sqrt{2}}$ and $|\eta_s\rangle = \Psi_{\eta_s}|s\bar{s}\rangle$, where Ψ_{η_i} $(i = q, s)$ denote the light-cone WFs of the corresponding parton states. Under such scheme, the decay constants in the quark-flavor basis simply follow the pattern of state mixing, i.e.,

$$\begin{pmatrix} f_\eta^q & f_\eta^s \\ f_{\eta'}^q & f_{\eta'}^s \end{pmatrix} = U(\phi)\mathrm{diag}[f_{\eta_q}, f_{\eta_s}], \tag{2}$$

where $f_{\eta_i} = (2\sqrt{3}) \int_{k_\perp^2 \le \mu_0^2} \frac{dx d^2k_\perp}{16\pi^3} \Psi_{\eta_i}(x, k_\perp)$ and the factorization scale $\mu_0 \sim \mathcal{O}(1\ \mathrm{GeV})$.

One can obtain the correlation between f_{η_q}/f_{η_s} and ϕ from the two-photon decay of η and η', i.e., $\eta/\eta' \to \gamma\gamma$, which shows [37] that

$$f_{\eta_q} = \frac{c_q \alpha}{8\pi^{3/2}} \left[\sqrt{\frac{\Gamma_{\eta\to\gamma\gamma}}{M_\eta^3}} \cos\phi + \sqrt{\frac{\Gamma_{\eta'\to\gamma\gamma}}{M_{\eta'}^3}} \sin\phi \right]^{-1} \tag{3}$$

and

$$f_{\eta_s} = \frac{c_s \alpha}{8\pi^{3/2}} \left[\sqrt{\frac{\Gamma_{\eta'\to\gamma\gamma}}{M_{\eta'}^3}} \cos\phi - \sqrt{\frac{\Gamma_{\eta\to\gamma\gamma}}{M_\eta^3}} \sin\phi \right]^{-1}, \tag{4}$$

where $c_s = \sqrt{2}/3$, $c_q = 5/3$, and $\alpha = 1/137$. Since the power-suppressed higher twist and higher helicity components give negligible contributions to the two-photon decay of η and η', the correlations (3) and (4) provide strong constraint on f_{η_q}, f_{η_s}, and ϕ.

B. Wave function of the light pseudoscalar meson

As for the light pseudoscalar meson (P), its light-cone WF can be written as

$$\Psi_P(x, \mathbf{k}_\perp) = \sum_{\lambda_1\lambda_2} \chi^{\lambda_1\lambda_2}(x, m_i, \mathbf{k}_\perp) \Psi_P^R(x, m_i, \mathbf{k}_\perp), \tag{5}$$

where i stands for the light quark q or s, and λ_1 and λ_2 are helicities of the two constituent quarks. $\chi^{\lambda_1\lambda_2}(x, \mathbf{k}_\perp)$ stands for the spin-space WF coming from the Wigner-Melosh rotation. $\Psi_{q\bar{q}}^R(x, m_i, \mathbf{k}_\perp)$ stands for the spatial WF, which can be factorized as [28]

$$\Psi_P^R(x, m_i, \mathbf{k}_\perp) = A\varphi_P(x) \exp\left[-\frac{\mathbf{k}_\perp^2 + m_i^2}{8\beta_i^2 x(1-x)} \right]. \tag{6}$$

The x-dependent $\varphi_P(x)$ can be expanded in Gegenbauer polynomials, and, by keeping its first two terms, we obtain

$$\Psi_P^R(x, m_i, \mathbf{k}_\perp) = A(1 + B \times C_2^{3/2}(2x-1)) \times \exp\left[-\frac{\mathbf{k}_\perp^2 + m_i^2}{8\beta^2 x(1-x)} \right]. \tag{7}$$

As for the parameters B and β, B determines the broadness of the WF in the longitudinal direction, while β determines the WF's transverse behavior.

The DA $\phi_P(x)$ can be obtained from $\Psi_P(x, \mathbf{k}_\perp)$ by integrating over the transverse momentum, $\phi_P(x) = \int_{|\mathbf{k}_\perp|<\mu_0} \frac{d^2\mathbf{k}_\perp}{16\pi^3} (\frac{2\sqrt{3}}{f_P}) \Psi_P(x, \mathbf{k}_\perp)$, and we obtain

$$\phi_P(x, \mu_0^2) = \frac{\sqrt{3} A m \beta}{2\sqrt{2}\pi^{3/2} f_P} \sqrt{x(1-x)} (1 + B \times C_2^{3/2}(2x-1)) \cdot \left(\mathrm{Erf}\left[\sqrt{\frac{m^2+\mu_0^2}{8\beta^2 x(1-x)}} \right] - \mathrm{Erf}\left[\sqrt{\frac{m^2}{8\beta^2 x(1-x)}} \right] \right), \tag{8}$$

where $\mathrm{Erf}(x) = \frac{2}{\sqrt{\pi}} \int_0^x e^{-t^2} dt$. $\phi_P(x, \mu_0^2)$ can be expanded in conventional Gegenbauer polynomials, whose moments

$$a_n(\mu_0^2) = \frac{\int_0^1 dx \phi_P(x, \mu_0^2) C_n^{3/2}(2x-1)}{\int_0^1 dx 6x(1-x)[C_n^{3/2}(2x-1)]^2}.$$

Numerically, we find that its second Gegenbauer moment $a_2(\mu_0^2)$ is close to B, i.e., the DA's behavior is dominated by B. Moreover, when $B \simeq 0.00$, its DA is asymptoticlike; and when $B \simeq 0.60$, its DA is CZ-like. This shows that $\phi_P(x, \mu_0^2)$ can mimic the DA behavior from asymptoticlike to CZ-like naturally. Then, by comparing the estimations for $B \in [0.00, 0.60]$ with the experimental data on various processes, one may decide which is the right DA behavior possessed by the light pseudoscalar mesons. Here, we do not discuss the flat DA, since it is hard to explain the meson-photon transition form factor's behavior around $Q^2 \sim 0$ and will meet an even more serious end-point problem than the CZ-like DA at $x \sim 0, 1$ [28].

C. Pseudoscalar-photon transition form factors

The pseudoscalar meson-photon transition form factors can be divided into two parts,

$$F_{P\gamma}(Q^2) = F_{P\gamma}^{(V)}(Q^2) + F_{P\gamma}^{(NV)}(Q^2), \tag{9}$$

where $F_{P\gamma}^{(V)}(Q^2)$ is the valence quark part, and $F_{P\gamma}^{(NV)}(Q^2)$ stands for the nonvalence quark part that is related to the higher Fock state of the pseudoscalar meson.

Under the light-cone perturbative QCD approach [10], and by keeping the $k_\perp$ corrections in both the hard-scattering amplitude and the WF, $F_{\pi\gamma}(Q^2)$ has been calculated up to NLO [46–51]. For pseudoscalar meson-photon transition form factors up to NLO, we have [28]

$$F_{P\gamma}^{(V)}(Q^2) = \frac{\sqrt{3} e_P}{4\pi^2} \int_0^1 \int_0^{x^2Q^2} \frac{dx}{xQ^2} \left[1 - \frac{C_F \alpha_s(Q^2)}{4\pi} \left(\ln \frac{Q^2}{xQ^2 + k_\perp^2} + 2\ln x + 3 - \frac{\pi^2}{3} \right) \right] \cdot \Psi_P(x, k_\perp^2) dk_\perp^2, \tag{10}$$

where $[dx] = dx dx' \delta(1 - x - x')$, $C_F = 4/3$, and $k_\perp = |\mathbf{k}_\perp|$. Also, e_P relates to the electric charge of the constituent quarks, $e_\pi = 1/3$, $e_{\eta_q} = 5/9$, and $e_{\eta_s} = \sqrt{2}/9$.

As for $F_{P\gamma}^{(NV)}(Q^2)$, we adopt the model suggested by Ref. [47], which is constructed based on the form factor's limiting behavior at both $Q^2 \to 0$ and $Q^2 \to \infty$, i.e.,

$$F_{P\gamma}^{(NV)}(Q^2) = \frac{\alpha}{(1 + Q^2/\kappa^2)^2}, \tag{11}$$

where $\alpha = \frac{1}{2} F_{P\gamma}(0)$, and $\kappa = \sqrt{-\frac{F_{P\gamma}(0)}{F_{P\gamma}^{(NV)'}(Q^2)|_{Q^2\to 0}}}$ with the first derivative of $F_{P\gamma}^{(NV)}(Q^2)$ over Q^2 in the limit $Q^2 \to 0$ takes the form

$$F_{P\gamma}^{(NV)'}(Q^2)|_{Q^2\to 0} = \frac{\sqrt{3} e_P}{8\pi^2} \left[\frac{\partial}{\partial Q^2} \int_0^1 \int_0^{x^2Q^2} \left(\frac{\Psi_P(x, k_\perp^2)}{x^2 Q^2} \right) dx dk_\perp^2 \right]_{Q^2\to 0}.$$

The same phenomenological model for $F_{P\gamma}^{(NV)}(Q^2)$ has also been adopted by Ref. [16], where instead a fixed input parameter $\Lambda \sim 1.1$ GeV is introduced to replace the parameter κ. Since the octet-singlet mixing scheme [44,45] is adopted by Ref. [16], it is reasonable to take the same Λ for π, η_8, and η_0. Under the present adopted quark-flavor mixing scheme, we will numerically obtain $\kappa \sim 1.1$–1.2 GeV for a pion and η_q, and $\kappa \sim 1.5$–1.6 GeV for η_s, where different κ is rightly caused by the $SU_f(3)$-breaking effect.

Moreover, under the quark-flavor mixing scheme, $\eta - \gamma$ and $\eta' - \gamma$ transition form factors are related with $F_{\eta_q\gamma}(Q^2)$ and $F_{\eta_s\gamma}(Q^2)$ through the following equations:

$$F_{\eta\gamma}(Q^2) = F_{\eta_q\gamma}(Q^2)\cos\phi - F_{\eta_s\gamma}(Q^2)\sin\phi \tag{12}$$

and

$$F_{\eta'\gamma}(Q^2) = F_{\eta_q\gamma}(Q^2)\sin\phi + F_{\eta_s\gamma}(Q^2)\cos\phi. \tag{13}$$

III. NUMERICAL RESULTS AND DISCUSSIONS

A. Input parameters

Two-photon decay widths of η and η' and their masses can be found in PDG [52]:

$$\Gamma_{\eta\to\gamma\gamma} = 0.510 \pm 0.026 \text{ KeV},$$
$$M_\eta = 547.853 \pm 0.024 \text{ MeV},$$
$$\Gamma_{\eta'\to\gamma\gamma} = 4.28 \pm 0.19 \text{ KeV},$$
$$M_{\eta'} = 957.78 \pm 0.06 \text{ MeV},$$

and $f_\pi = 92.4 \pm 0.25$ MeV.

A weighted average of the experimental values shown in Ref. [53], together with two experimental values $\phi = 38.8° \pm 1.2°$ [35] and $\phi = 41.2° \pm 1.1°$ [54], yields

TABLE I. Typical WF parameters for $m_q = 0.30$ GeV and $m_s = 0.45$ GeV, where $\phi = 39.5°$ is adopted.

$B\|m$	β_π (GeV)	A_π (GeV^{-1})	A_q (GeV^{-1})	A_s (GeV^{-1})
$0.00\|m_q$	0.586	25.06	26.81	
$0.30\|m_q$	0.668	20.26	21.67	
$0.60\|m_q$	0.745	16.62	17.78	
$0.00\|m_s$	0.464	42.23		60.58
$0.30\|m_s$	0.504	36.97		49.58
$0.60\|m_s$	0.552	31.24		40.72

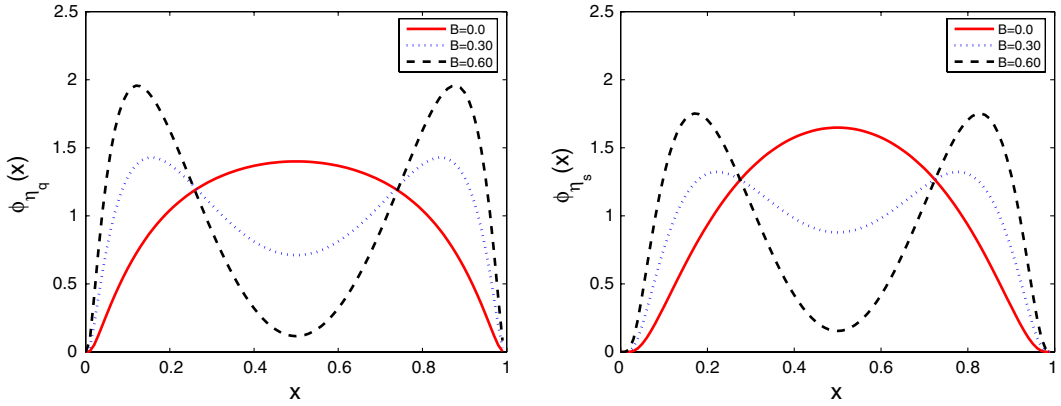

FIG. 1 (color online). DA model [Eq. (8)] for $\phi_{\eta_q}(x)$ (left) and $\phi_{\eta_s}(x)$ (right), with $\mu_0 = 1$ GeV, where $B = 0.00$, 0.30, and 0.60, respectively.

$\bar{\phi} = 39.5° \pm 0.5°$. Then, with the help of Eqs. (3) and (4), we obtain

$$f_{\eta_q}/f_\pi = 1.07 \pm 0.03 \tag{14}$$

and

$$f_{\eta_s}/f_\pi = 1.44 \pm 0.08, \tag{15}$$

which are consistent with the phenomenological values, $f_{\eta_q} \simeq f_\pi$ and $f_{\eta_s} \simeq 1.36 f_\pi$ [53].

As for the pion WF, its parameters can be determined by its normalization condition and the constraint from $\pi_0 \to \gamma\gamma$. A detailed determination of pion WF parameters can be found in Ref. [28], where β_π for the specified B and quark mass is determined by

$$\frac{\int_0^1 dx \int_{|\mathbf{k}_\perp|^2<\mu_0^2} \frac{d^2\mathbf{k}_\perp}{16\pi^3} \Psi_\pi(x, \mathbf{k}_\perp)}{\int_0^1 dx \Psi_\pi(x, \mathbf{k}_\perp = 0)} = \frac{f_\pi^2}{6}. \tag{16}$$

Because η_q and η_s have behaviors similar to that of π, for clarity, we take $\beta_q = \beta_\pi|_{m_q}$ and $\beta_s = \beta_\pi|_{m_s}$. Under the condition of $B = 0.00$, 0.30, and 0.60, typical parameters for the DAs of π, η_q, and η_s are presented in Table I, where the mixing angle ϕ is fixed to be 39.5°.

It is noted that, by varying B within the region of $\sim[0.00, 0.60]$, the DAs vary from asymptoticlike to CZ-like form. To show this point more clearly, we draw $\phi_{\eta_q}(x)$ and $\phi_{\eta_s}(x)$ in Fig. 1, where $B = 0.00$, 0.30, and 0.60, respectively.

B. Basic numerical results

Numerically, one may observe that, in the large Q^2 region, the leading valence Fock-state contribution dominates the form factor $Q^2 F_{P\gamma}(Q^2)$, while the nonvalence quark part $Q^2 F_{P\gamma}^{\rm NV}(Q^2)$ is power suppressed and is quite small, so it is usually neglected in the literature. However, $Q^2 F_{P\gamma}^{\rm NV}(Q^2)$ can provide sizable contributions in the low- and intermediate-energy regions, so one should take it into consideration to make a more sound estimation over all of the energy regions.

As shown above, the parameter B in the unified WF model (5) determines the DA behavior of the light pseudoscalar mesons. Then, by comparing with the experimental data on the pseudoscalar meson-photon transition form factors, we have the opportunity to discuss the DA properties in a more consistent way.

First, we present the meson-photon transition form factors within a wide region of $B \in [0.00, 0.60]$ so as to show which DA behavior is more suitable to explain the data, especially the *BABAR* data [14]. In doing the numerical calculation, we take all the other input parameters to be their center values, i.e., $m_q = 0.30$ GeV, $m_s = 0.45$ GeV, and $\phi = 39.5°$. Figures 2 and 3 show the pseudoscalar-photon transition form factors $Q^2 F_{\pi\gamma}(Q^2)$, $Q^2 F_{\eta\gamma}(Q^2)$, and $Q^2 F_{\eta'\gamma}(Q^2)$, where $B = 0.00$, 0.30 and 0.60, respectively. These two figures show that, with the increment of B, all three form factors decrease in the lower Q^2 region but increase in the higher Q^2 region. Especially noteworthy

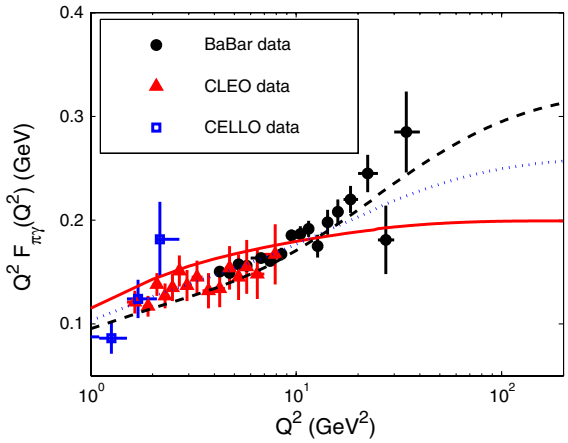

FIG. 2 (color online). $\pi - \gamma$ transition form factor $Q^2 F_{\pi\gamma}(Q^2)$ with varying B. The solid, dotted, and dashed lines are for $B = 0.00$, 0.30, and 0.60, respectively. The experimental data are taken from Refs. [12–14].

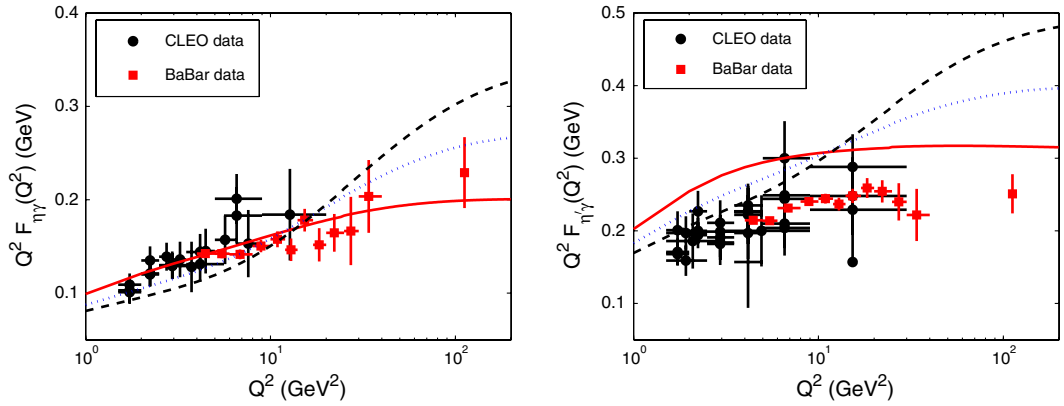

FIG. 3 (color online). $\eta - \gamma$ (left) and $\eta' - \gamma$ (right) transition form factors $Q^2 F_{\eta\gamma}(Q^2)$ and $Q^2 F_{\eta'\gamma}(Q^2)$. The solid, dotted, and dashed lines are for $B = 0.00$, 0.30, and 0.60, respectively. The experimental data are taken from Refs. [13,33,36].

is that the CZ-like DA ($B = 0.60$) leads to the smallest value in the lower Q^2 region, while the AS-like DA ($B = 0.00$) leads to the biggest value; in the higher Q^2 region, the conditions are vice versa. This creates the puzzle of how to explain the newly obtained *BABAR* data on the $\pi - \gamma$ form factor. The *BABAR* data show that, in the range of $Q^2 \in [4, 40]$ GeV^2, the pion-photon transition form factor behaves as [14] $Q^2 F_{\pi\gamma}(Q^2) = A(\frac{Q^2}{10\ \mathrm{GeV}^2})^{\beta}$, where $A = 0.182 \pm 0.002$ and $\beta = 0.25 \pm 0.02$. A CZ-like DA with $B \sim 0.60$ or even a flat DA can explain the data well for the higher Q^2 region,[1]; however, they fail in the lower Q^2 region. The AS-like DA with $B \sim 0.00$ provides a better understanding for the lower Q^2 region, but because $Q^2 F_{\pi\gamma}(Q^2)$ tends to be a constant value ($2f_\pi$), it cannot explain the large Q^2 behavior. On the one hand, by increasing B from 0 to a larger value, the estimated large-Q^2 behavior of $Q^2 F_{\pi\gamma}(Q^2)$ can be improved. On the other hand, the deviation of the lower-Q^2 behavior also increases with the increment of B, so B should not be too large. Moreover, as shown by Fig. 3, the $\eta - \gamma$ form factor $Q^2 F_{\eta\gamma}(Q^2)$ prefers a DA with smaller B, i.e., $B \lesssim 0.30$. For the $\eta' - \gamma$ form factor $Q^2 F_{\eta'\gamma}(Q^2)$, all DAs lead to large-Q^2 behavior well above the experimental data.

Second, we study the uncertainties of the transition form factors caused by m_q and m_s. For this purpose, we take $m_q = 0.30 \pm 0.05$ GeV and $m_s = 0.45 \pm 0.05$ GeV, and we fix the parameter $B = 0.30$ and $\phi = 39.5°$. The $\pi - \gamma$ form factor for $m_q = 0.30 \pm 0.05$ GeV is presented in Fig. 4. Figure 5 presents the $\eta - \gamma$ and $\eta' - \gamma$ form factors for $m_q = 0.25$ GeV and $m_s = 0.40$ GeV; $m_q = 0.30$ GeV and $m_s = 0.45$ GeV; and $m_q = 0.35$ GeV and $m_s = 0.50$ GeV. It can be found that the form factors change with the constituent quark mass, similar to their change with B. That is, with the increment of constituent quark

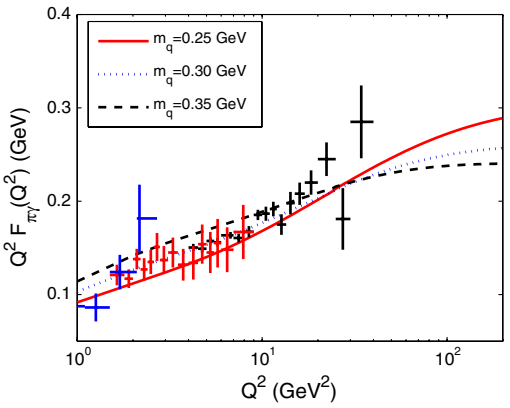

FIG. 4 (color online). $\pi - \gamma$ transition form factor $Q^2 F_{\pi\gamma}(Q^2)$ with fixed $B = 0.3$. The solid [red] line, dotted [blue] line, and dashed black line are for $m_q = 0.25$ GeV, 0.30 GeV, and 0.35 GeV, respectively. The experimental data are taken from Refs. [12–14].

mass, all three form factors increase in the lower Q^2 region and decrease in the higher Q^2 region. Naïvely, one may expect to obtain a larger high-Q^2 behavior by setting a smaller m_q and m_s. Especially by setting the limiting values of $m_q = 0$ and $B = 0$, which rightly correspond to a flat φ_π as suggested by Ref. [22], one can obtain the same logarithmic behavior for the large Q^2 region that is consistent with *BABAR* data, i.e., $Q^2 F_{\pi\gamma}(Q^2) \propto \ln(Q^2/2\sigma^2)$ with $\sigma = \frac{M_0^2}{2} e^{\gamma_E}$. However, it is found that m_q cannot be too small; i.e., it should be larger than 0.22 GeV, because otherwise the probability of the leading valence quark state $|q\bar{q}\rangle$ will be larger than 1 [55].

The conditions for $\eta - \gamma$ and $\eta' - \gamma$ are somewhat different. Because of $\eta - \eta'$ mixing, we need to consider these two form factors simultaneously. The curves for $Q^2 F_{\eta\gamma}(Q^2)$ and $Q^2 F_{\eta'\gamma}(Q^2)$ for $\phi = 39.5° \pm 0.5°$ are presented in Fig. 6. It is found that $Q^2 F_{\eta\gamma}(Q^2)$ decreases with the increment of ϕ, while $Q^2 F_{\eta'\gamma}(Q^2)$ increases

[1]The form factor with flat DA leads to logarithmic growth with Q^2, i.e., $Q^2 F_{\pi\gamma}(Q^2) \propto \ln(1 + Q^2/M^2)$ [22], which is close to the *BABAR* data.

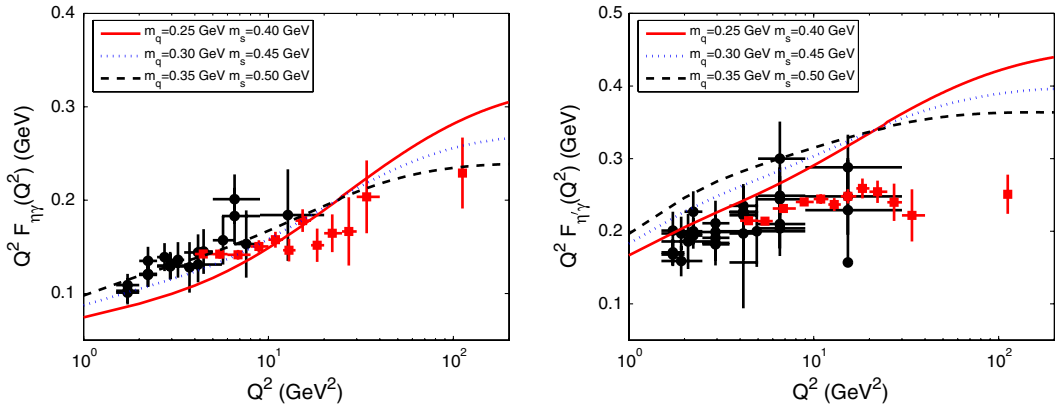

FIG. 5 (color online). $\eta - \gamma$ (left) and $\eta' - \gamma$ (right) transition form factors $Q^2 F_{\eta\gamma}(Q^2)$ and $Q^2 F_{\eta'\gamma}(Q^2)$ with fixed $B = 0.3$ and $\phi = 39.5°$. The solid [red] line, the dotted [blue] line, and the dashed black line are for [$m_q = 0.25$ GeV and $m_s = 0.40$ GeV], [$m_q = 0.30$ GeV and $m_s = 0.45$ GeV], and [$m_q = 0.35$ GeV and $m_s = 0.50$ GeV], respectively. The experimental data are taken from Refs. [13,33,36].

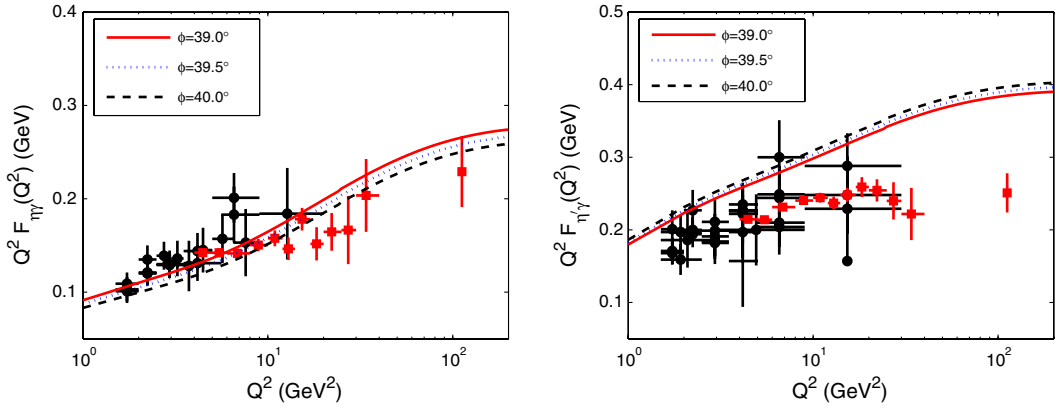

FIG. 6 (color online). $\eta - \gamma$ (left) and $\eta' - \gamma$ (right) transition form factors $Q^2 F_{\eta\gamma}(Q^2)$ and $Q^2 F_{\eta'\gamma}(Q^2)$ with fixed $B = 0.3$, and with $m_q = 0.30$ GeV and $m_s = 0.45$ GeV. The experimental data are taken from Refs. [13,33,36].

with the increment of ϕ. By shifting ϕ to a smaller value $\sim 38°$, one can explain these two form factors within $Q^2 < 20$ GeV^2 consistently, as has been pointed out by Ref. [37]. However, such a shifting of ϕ cannot explain the new *BABAR* data on $\eta - \gamma$ and $\eta' - \gamma$ for even larger $Q^2 > 20$ GeV^2. So it is hard to fit the gap between the theoretical estimation and the experimental data in the whole Q^2 region by a simple variation of ϕ. Experimentally, $Q^2 F_{\eta\gamma}(Q^2)$ still increases with the increment of Q^2 up to a large value even though its ascending trends are slower than the growth of $Q^2 F_{\pi\gamma}(Q^2)$, while $Q^2 F_{\eta'\gamma}(Q^2)$ tends to be consistent for $Q^2 \to \infty$. So some other sources must be introduced to explain both the $\eta - \gamma$ and $\eta' - \gamma$ form factors in the whole energy region consistently. As shown by Fig. 3, $Q^2 F_{\eta\gamma}(Q^2)$ can agree with the data with $B \sim 0.30$, so we hope the new sources will have less effect on $Q^2 F_{\eta\gamma}(Q^2)$ than on $Q^2 F_{\eta'\gamma}(Q^2)$. It has been suggested that a proper intrinsic charm component may be some help in explaining the abnormally large production of η' [53,56–58]. In the following subsection, we will give a detailed discussion on possible contributions from the intrinsic charm components.

C. Possible contributions from the intrinsic charm components to $Q^2 F_{\eta\gamma}(Q^2)$ and $Q^2 F_{\eta'\gamma}(Q^2)$

Since the mixing between the $c\bar{c}$ state with $q\bar{q}$-$s\bar{s}$ basis is quite small [53], we can set

$$F_{\eta\gamma}(Q^2) = F_{\eta_q\gamma}(Q^2)\cos\phi - F_{\eta_s\gamma}(Q^2)\sin\phi + F^{\eta}_{\eta_c\gamma}(Q^2), \tag{17}$$

$$F_{\eta'\gamma}(Q^2) = F_{\eta_q\gamma}(Q^2)\sin\phi + F_{\eta_s\gamma}(Q^2)\cos\phi + F^{\eta'}_{\eta_c\gamma}(Q^2), \tag{18}$$

where $F^{\eta}_{\eta_c\gamma}(Q^2)$ and $F^{\eta'}_{\eta_c\gamma}(Q^2)$ correspond to the contributions from the intrinsic charm component in η and η', respectively. Similarly, the WF of the intrinsic charm component $\eta_c = |c\bar{c}\rangle$ can be modeled as

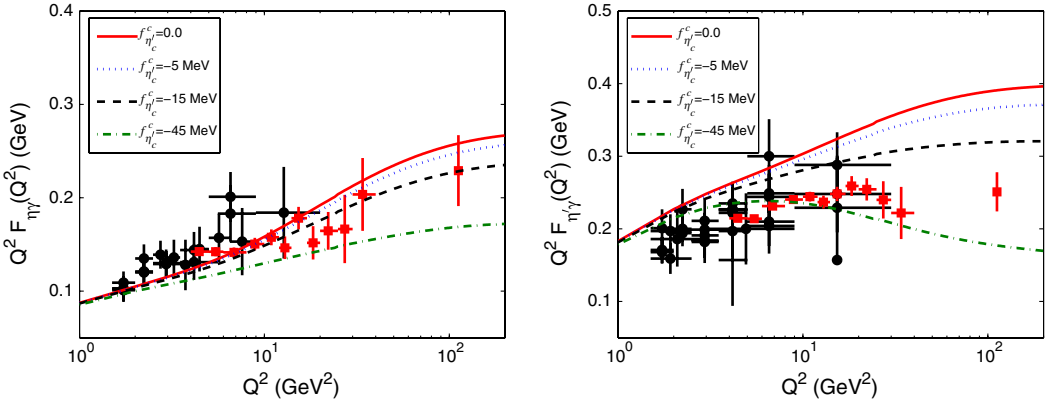

FIG. 7 (color online). $\eta-\gamma$ (left) and $\eta'-\gamma$ (right) transition form factors $Q^2F_{\eta\gamma}(Q^2)$ and $Q^2F_{\eta'\gamma}(Q^2)$ with varying $f^c_{\eta'}$, where we take $B=0.30$, $m_q=0.30$ GeV, $m_s=0.45$ GeV, and $m_c=1.50$ GeV. The experimental data are taken from Refs. [13,33,36].

$$\Psi^c_{\eta/\eta'}(x,\mathbf{k}_\perp)=A^c_{\eta/\eta'}(1+B\times C_2^{3/2}(2x-1))\times\left[\exp\left(-\frac{\mathbf{k}_\perp^2+m_c^2}{8\beta_c^2x(1-x)}\right)\chi^K(m_c,x,\mathbf{k}_\perp)\right], \tag{19}$$

where we adopt $\beta_c=\beta_\pi|_{m_c}$. The overall factor $A^c_{\eta/\eta'}$ is determined by the WF normalization, in which their corresponding decay constants f^c_η and $f^c_{\eta'}$ are related by $\frac{f^c_\eta}{f^c_{\eta'}}=-\tan[\phi-\arctan\frac{\sqrt{2}f_s}{f_q}]$ [53]. Here, to calculate $F^\eta_{\eta_c\gamma}(Q^2)$ and $F^{\eta'}_{\eta_c\gamma}(Q^2)$, the charm-quark mass effect should be taken into consideration in the hard part of the amplitude, i.e., the higher helicity states that are proportional to the quark mass will provide sizable contributions. After integrating over the azimuth angle, a direct calculation shows [37]

$$Q^2F_{\eta_c\gamma}(Q^2)=\frac{\sqrt{2}}{3\sqrt{3}\pi^2}\int_0^1\frac{dx}{x}\int_0^\infty\Psi^c_{\eta/\eta'}(x,k_\perp^2)\times\left[1+\frac{1-z-y^2}{\sqrt{(z+(1-y)^2)(z+(1+y)^2)}}\right]k_\perp dk_\perp, \tag{20}$$

where $z=\frac{m_c^2}{x^2Q^2}$ and $y=\frac{k_\perp}{xQ}$.

Taking $B=0.30$, $m_q=0.30$ GeV, $m_s=0.45$ GeV, $m_c=1.50$ GeV, and $\phi=39.5°$, we show how $f^c_{\eta'}$ affects the form factors $Q^2F_{\eta\gamma}(Q^2)$ and $Q^2F_{\eta'\gamma}(Q^2)$. The results are presented in Fig. 7, where $f^c_{\eta'}=0$, -5 MeV, -15 MeV, and -45 MeV, respectively. These two form factors are slightly affected by the charm component in the low Q^2 region, while in the high Q^2 region, the form factors are quite sensitive to $f^c_{\eta'}$ and they can be greatly suppressed by a possible charm component. One may observe that the experimental data disfavors a larger portion of charm component as $|f^c_{\eta'}|\gtrsim 50$ MeV. And for even larger $|f^c_{\eta'}|$, the data have more obvious effects on $Q^2F_{\eta'\gamma}(Q^2)$ than on $Q^2F_{\eta\gamma}(Q^2)$, which is what we wanted.

Moreover, we present the results for $\eta-\gamma$ and $\eta'-\gamma$ transition form factors with fixed $f^c_{\eta'}=-30$ MeV in Fig. 8, where $B=0.0$, 0.30 and 0.60, respectively. It shows that, with a proper charm component $f^c_{\eta'}\sim-30$ MeV and $B\sim 0.30$, the experimental data on $Q^2F_{\eta\gamma}(Q^2)$ and $Q^2F_{\eta'\gamma}(Q^2)$ can be consistently explained. It is found

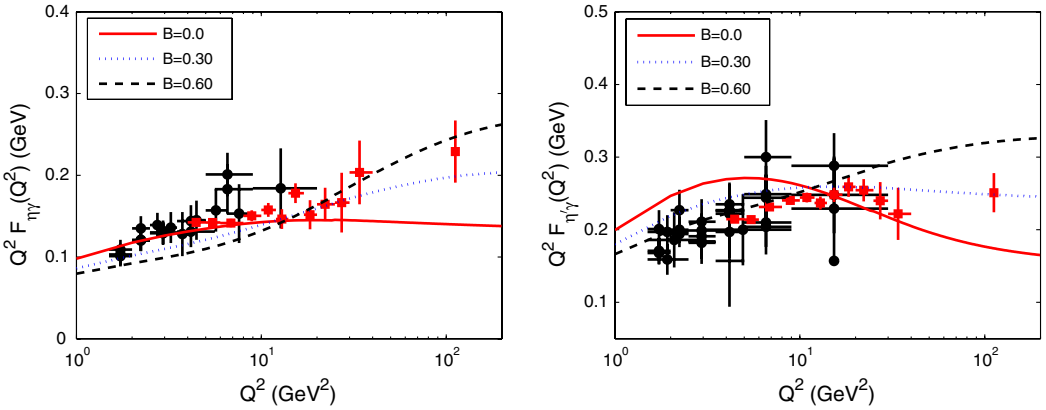

FIG. 8 (color online). $\eta-\gamma$ (left) and $\eta'-\gamma$ (right) transition form factors $Q^2F_{\eta\gamma}(Q^2)$ and $Q^2F_{\eta'\gamma}(Q^2)$ with varying B, where $f^c_{\eta'}=-30$ MeV, $m_q=0.30$ GeV, $m_s=0.45$ GeV, and $m_c=1.50$ GeV. The experimental data are taken from Refs. [13,33,36].

that $f^c_{\eta'} = -30$ MeV is consistent with Refs. [41,58]. Because we still have $|f^c_{\eta'}| \ll f_{\eta_c} \sim 400$ MeV, according to the mass-matrix-element shown by Ref. [53], we still have $M_{\eta_c} \simeq m_{cc}$ up to high accuracy. And applying the parameters to the formulas presented in Ref. [53], it can be found that the mixing between $c\bar{c}$ state with $q\bar{q} - s\bar{s}$ basis is still quite small, i.e., the mixing is around 1%. Thus our present approximations (17) and (18) are still reasonable.

IV. SUMMARY

The light pseudoscalar meson-photon transition form factor provides a good platform for studying the leading-twist DA of the light pseudoscalar mesons since it contains only one bound state. In the present paper, we have analyzed three pseudoscalar meson-photon transition form factors consistently by using a uniform WF model suggested by Ref. [28]. By comparing the estimations with the experimental data on these form factors, it can provide strong constraints on the light pseudoscalar meson DAs. Our results are listed in this summary:

(1) According to Eqs. (9)–(11), all pseudoscalar meson-photon transition form factors $Q^2F_{\pi\gamma}(Q^2)$, $Q^2F_{\eta_q\gamma}(Q^2)$, and $Q^2F_{\eta_s\gamma}(Q^2)$ should have similar behaviors. Since no growth of $Q^2F_{\eta\gamma}(Q^2)$ and $Q^2F_{\eta'\gamma}(Q^2)$ as rapid as that of $Q^2F_{\pi\gamma}(Q^2)$ has been found experimentally, these first two form factors can be explained by setting $B \sim 0.30$ together with a small charm quark component $|f^c_{\eta'}| \sim 30$ MeV. Such a moderate DA with $B \sim 0.30$ for η_q and η_s, which corresponds to the second Gegenbauer DA moment around 0.35, may also be the pion DA behavior.

(2) We have discussed in detail the form factors' uncertainties caused by the constituent quark masses m_q and m_s, the parameter B, the mixing angle ϕ, and the possible intrinsic charm components f^c_η and $f^c_{\eta'}$. First, the parameter B determines the main behavior of the form factors. By varying $B \in [0.00, 0.60]$, one can conveniently compare the results for the $\pi - \gamma$ transition form factor with those obtained in the literature, in which DA behavior varies from AS-like to CZ-like, accordingly. A CZ-like DA with $B \sim 0.60$ can explain the data in the high Q^2 region; however, it fails to explain the form factors' lower-Q^2 behavior. While the AS-like DA with $B \sim 0.00$ can give a better understanding for the lower Q^2 region, it cannot explain the present *BABAR* data for large Q^2 behavior. Second, the parameters m_q, m_s, and ϕ can improve the behavior slightly. With the increment of m_q and m_s, three form factors $Q^2F_{\pi\gamma}(Q^2)$, $Q^2F_{\eta\gamma}(Q^2)$, and $Q^2F_{\eta'\gamma}(Q^2)$ increase in the lower Q^2 region and decrease in the higher Q^2 region. $Q^2F_{\eta\gamma}(Q^2)$ decreases with the increment of ϕ, while $Q^2F_{\eta'\gamma}(Q^2)$ increases with the increment of ϕ. Third, $Q^2F_{\eta\gamma}(Q^2)$ and $Q^2F_{\eta'\gamma}(Q^2)$ are slightly affected by the charm component in the low Q^2 region, while in the high Q^2 region, the form factors are quite sensitive to $f^c_{\eta'}$, and they can be greatly suppressed by the possible charm component.

(3) It has been found that, by adjusting these parameters within their reasonable regions, one can improve the estimates of the form factors to a certain degree but still cannot solve the puzzle, especially to explain the behavior of the $\pi - \gamma$ form factor within the whole Q^2 region consistently. Because of the cancellation between $F_{\eta_q\gamma}$ and $F_{\eta_s\gamma}$, it is reasonable that $Q^2F_{\eta'\gamma}(Q^2)$ tends to be a constant as $Q^2 \to \infty$ [33,36]. However, it is hard to understand why $Q^2F_{\eta\gamma}(Q^2)$ and $Q^2F_{\pi\gamma}(Q^2)$ have such a quite-different large Q^2 behavior. It is especially hard to explain the rapid growth of $Q^2F_{\pi\gamma}(Q^2)$, which is probably the logarithmic growth [21,22], reported by the *BABAR* Collaboration [14] to be consistent with the previously obtained low Q^2 behavior by the CELLO and CLEO collaborations [12,13]. Possible charm components f^c_η and $f^c_{\eta'}$ can shrink the gap between these two form factors to a certain degree, but they cannot be the reason for such a large difference. We hope that more experimental data on these form factors in the large Q^2 region can clarify the present situation. If the *BABAR* data is confirmed, then they may indeed indicate new physics in these form factors, since it is hard to explain using the currently adopted light-cone pQCD framework.

ACKNOWLEDGMENTS

This work was supported in part by the Fundamental Research Funds for the Central Universities under Grant No. CDJZR101000616, the Program for New Century Excellent Talents in University under Grant No. NCET-10-0882, and by the Natural Science Foundation of China under Grants No. 10975144, No. 10805082, and No. 11075225.

[1] T. Huang, B. Q. Ma, and Q. X. Shen, Phys. Rev. D **49**, 1490 (1994); T. Huang and X. G. Wu, Phys. Rev. D **70**, 093013 (2004); X. G. Wu, Eur. Phys. J. C **57**, 665 (2008).

[2] V. M. Braun, A. Khodjamirian, and M. Maul, Phys. Rev. D **61**, 073004 (2000).

[3] A. P. Bakulev, S. V. Mikhailov, and N. G. Stefanis, Phys. Lett. B **578**, 91 (2004); A. P. Bakulev, K. Passek-Kumericki, W. Schroers, and N. G. Stefanis, Phys. Rev. D **70**, 033014 (2004); **70**, 079906(E) (2004); A. P. Bakulev, S. V. Mikhailov, and N. G. Stefanis, Phys. Rev. D **67**, 074012 (2003); **73**, 056002 (2006).

[4] P. Ball and R. Zwicky, Phys. Lett. B **625**, 225 (2005).

[5] Seung-il Nam, Hyun-Chul Kim, Atsushi Hosaka, and M. M. Musakhanov, Phys. Rev. D **74**, 014019 (2006).

[6] S. S. Agaev, Phys. Rev. D **72**, 114010 (2005); **73**, 059902 (E) (2006).

[7] L. Del Debbio, M. Di Perro, and A. Dougall, Nucl. Phys. B, Proc. Suppl. **119**, 416 (2003).

[8] M. Gockeler *et al.*, Nucl. Phys. B, Proc. Suppl. **161**, 69 (2006).

[9] S. Dalley and Brett van de Sande, Phys. Rev. D **67**, 114507 (2003).

[10] G. P. Lepage and S. J. Brodsky, Phys. Rev. D **22**, 2157 (1980).

[11] V. L. Chernyak and A. R. Zhitnitsky, Nucl. Phys. **B201**, 492 (1982).

[12] H.-J. Behrend *et al.* (CELLO Collaboration), Z. Phys. C **49**, 401 (1991).

[13] V. Savinov *et al.* (CLEO Collaboration), arXiv:hep-ex/9707028; J. Gronberg *et al.* (CLEO Collaboration), Phys. Rev. D **57**, 33 (1998).

[14] B. Aubert *et al.* (*BABAR* Collaboration), Phys. Rev. D **80**, 052002 (2009).

[15] E. R. Arriola and W. Broniowski, Phys. Rev. D **66**, 094016 (2002).

[16] S. J. Brodsky, F. G. Cao, and Guy F. de Téramond, Phys. Rev. D **84**, 033001 (2011).

[17] S. J. Brodsky, F. G. Cao, and Guy F. de Téramond, arXiv:1105.3999 [Phys. Rev. D (to be published)].

[18] S. V. Mikhailov, A. V. Pimikov, and N. G. Stefanis, Phys. Rev. D **82**, 054020 (2010).

[19] M. K. Gawenda and A. Szczurek, Phys. Lett. B **700**, 322 (2011).

[20] A. P. Bakulev, S. V. Mikhailov, A. V. Pimikov, and N. G. Stefanis, Phys. Rev. D **84**, 034014 (2011).

[21] F. Zuo and T. Huang, arXiv:1105.6008.

[22] A. V. Radyushkin, Phys. Rev. D **80**, 094009 (2009).

[23] S. S. Agaev, V. M. Braun, N. Offen, and F. A. Porkert, Phys. Rev. D **83**, 054020 (2011).

[24] P. Kroll, Eur. Phys. J. C **71**, 1623 (2011).

[25] O. Leitner, J. F. Mathiot, and N. A. Tsirova, Eur. Phys. J. A **47**, 17 (2011).

[26] S. Noguera and V. Vento, Eur. Phys. J. A **46**, 197 (2010).

[27] E. R. Arriola and W. Broniowski, Phys. Rev. D **81**, 094021 (2010).

[28] X. G. Wu and T. Huang, Phys. Rev. D **82**, 034024 (2010).

[29] H. Aihara *et al.* (TPC/Two-Gamma Collaboration), Phys. Rev. Lett. **64**, 172 (1990).

[30] M. Acciarri *et al.* (L3 Collaboration), Phys. Lett. B **418**, 399 (1998).

[31] A. Aloisio *et al.* (KLOE Collaboration), Phys. Lett. B **541**, 45 (2002).

[32] S. E. Muller *et al.* (KLOE Collaboration), Int. J. Mod. Phys. A **20**, 1888 (2005).

[33] B. Aubert *et al.* (*BABAR* Collaboration), Phys. Rev. D **74**, 012002 (2006).

[34] C. Berger *et al.* (PLUTO Collaboration), Phys. Lett. B **142**, 225 (1984).

[35] M. Ablikim *et al.* (BES Collaboration), Phys. Rev. D **73**, 052008 (2006).

[36] P. del Amo Sanchez *et al.* (*BABAR* Collaboration), Phys. Rev. D **84**, 052001 (2011).

[37] T. Huang and X. G. Wu, Eur. Phys. J. C **50**, 771 (2007).

[38] S. S. Agaev, Eur. Phys. J. C **70**, 125 (2010).

[39] S. S. Agaev and N. G. Stefanis, Phys. Rev. D **70**, 054020 (2004).

[40] F. G. Cao and A. I. Signal, Phys. Rev. D **60**, 114012 (1999).

[41] T. Feldmann and P. Kroll, Eur. Phys. J. C **5**, 327 (1998).

[42] M. K. Chase, Nucl. Phys. **B174**, 109 (1980); T. Ohrndorf, Nucl. Phys. **B186**, 153 (1981).

[43] S. S. Agaev, Phys. Rev. D **64**, 014007 (2001).

[44] T. Feldmann, Int. J. Mod. Phys. A **15**, 159 (2000).

[45] T. Feldmann, Nucl. Phys. B, Proc. Suppl. **74**, 151 (1999).

[46] S. J. Brodsky, T. Huang, and G. P. Lepage, in *Particles and Fields 2: Proceedings of the Banff Summer Institute, Banff, Alberta, 1981*, edited by A. Z. Capri and A. N. Kamal (Plenum, New York, 1983), p. 143; T. Huang, in *Proceedings of XXth International Conference on High Energy Physics, Madison, Wisconsin, 1980*, edited by L. Durand and L. G. Pondrom, AIP Conf. Proc. No. 69 (AIP, New York, 1981), p. 1000.

[47] T. Huang and X. G. Wu, Int. J. Mod. Phys. A **22**, 3065 (2007).

[48] Fu-Guang Cao, Tao Huang, and Bo-Qiang Ma, Phys. Rev. D **53**, 6582 (1996); Tao Huang and Qi-Xing Shen, Z. Phys. C **50**, 139 (1991).

[49] S. Nandi and H. N. Li, Phys. Rev. D **76**, 034008 (2007).

[50] H. N. Li and S. Mishima, Phys. Rev. D **80**, 074024 (2009).

[51] I. V. Musatov and A. V. Radyushkin, Phys. Rev. D **56**, 2713 (1997).

[52] K. Nakamura *et al.* (Particle Data Group), J. Phys. G **37**, 075021 (2010).

[53] T. Feldmann, P. Kroll, and B. Stech, Phys. Rev. D **58**, 114006 (1998).

[54] P. Kroll, Mod. Phys. Lett. A **20**, 2667 (2005).

[55] T. Huang, X. G. Wu, and X. H. Wu, Phys. Rev. D **70**, 053007 (2004); X. G. Wu and T. Huang, Int. J. Mod. Phys. A **21**, 901 (2006).

[56] I. Halperin and A. Zhitnitsky, Phys. Rev. D **56**, 7247 (1997); H. Y. Cheng and B. Tseng, Phys. Lett. B **415**, 263 (1997).

[57] T. W. Yeh, Phys. Rev. D **65**, 094019 (2002).

[58] Feng Yuan and Kuang-Ta Chao, Phys. Rev. D **56**, R2495 (1997).